# Electrochemical Deposition of $BaSO_4$ Coatings on Stainless Steel Substrates

M. Dinamani,† P. Vishnu Kamath,† and Ram Seshadri*,‡

*Department of Chemistry, Central College, Bangalore University, Bangalore 560 001, India, and Solid State and Structural Chemistry Unit, Indian Institute of Science, Bangalore 560 012, India*

Adherent $BaSO_4$ coatings have been electrochemically deposited on anode substrates from aqueous solution for the first time by electrogeneration of acid. At low current densities, thick, nearly continuous coatings comprising unoriented crystallites are obtained. At higher current densities, the coatings are not as continuous but the crystallites are oriented. At short deposition times and under high current densities, the crystallites are oriented with the *a* axis perpendicular to the substrate. At long deposition times, the orientation switches to the *c* axis. Electroless deposition under similar conditions yields crystallites that are neither oriented nor facetted.

## Introduction

Barium sulfate ($BaSO_4$ space group *Pnma*, $a = 8.8701$ Å; $b = 5.4534$ Å; $c = 7.1507$ Å) is a structural analogue of the ubiquitous biomineral aragonite ($CaCO_3$). The latter is found deposited in a number of biological systems, stabilized in conjunction with structure-directing biomolecules, which are known to act by a process of molecular recognition of specific crystal faces.[1,2] $BaSO_4$ differs from $CaCO_3$ in that it possesses tetrahedral sulfate moieties in place of the planar carbonate anions. Consequently, crystal growth of $BaSO_4$ has been studied as a model to probe the relative structure and growth-directing efficacies of carboxylates, phosphonates, sulfonates, and other organic template molecules.[3] $BaSO_4$ particles with unusual sizes, shapes, texture, and morphology have been synthesized by designing suitable organic templates.[4,5] $BaSO_4$ together with $CaCO_3$ is also found deposited in the scales in industrial water transport systems, and as a result, methods of inhibiting its nucleation and growth have received much attention. Morizot and Neville[6] have used electrochemistry as an analytical tool to estimate the chemical growth of $BaSO_4$ scales and their suppression in the presence of commercial inhibitors. Crystal growth inhibitors also act through molecular recognition by bonding to the fast growing faces of $BaSO_4$ crystallites and inhibiting growth.[3] Crystal growth inhibitors thereby promote growth along other directions.[7] $BaSO_4$ has been used as a model system to test different theories of crystal growth.[8]

We have for some time been interested in the uses of electrochemistry to synthesize inorganic materials.[9] Electrochemical synthesis has many features in common with template/additive mediated synthesis: (i) The electrode itself behaves as a template with the solid-phase depositing on it as a film or a coating. In this the electrode serves an important role in breaking the continuous symmetry of the solution. (ii) Crystal growth is initiated in the electric double layer, which has a high potential gradient on the order of $10^5-10^7$ V/cm. This potential gradient can assist in directing the crystal growth. (iii) The deposition current is a measure of the crystal growth rate and can be finely controlled.

Electrochemical synthesis has been employed to obtain oriented,[10] epitaxial,[11] compositionally modulated,[12] and nanostructured thin films of metal oxides.[13] The first application of electrosynthesis to the preparation of an inorganic biomaterial was for the synthesis of calcium phosphates.[14,15] Subsequently, Melendres and co-workers studied the deposition of pure and Mg-containing $CaCO_3$ coatings and investigated the structure of the deposit as a function of the $Mg^{2+}$ concentration.[16]

The precipitation of most inorganic materials requires dehydration of the solvation spheres from around the cations. This is favored at high pH, so most electrosynthesis of inorganic materials takes place at the cathode, where there is electrogeneration of base. Exceptions arise when anodic oxidation is used as a tool to

† Bangalore University.
‡ Indian Institute of Science.

(1) Mann, S.; Heywood, B. R.; Rajam, S.; Birchall, J. D. *Nature* **1988**, *334*, 692.
(2) Mann, S.; Didymus, J. M.; Sanderson, N. P.; Heywood, B. R.; Aso Samper, E. J. *J. Chem. Soc., Faraday Trans.* **1990**, *86*, 1873.
(3) Davey, R. J.; Black, S. N.; Bromley, L. A.; Cottier, D.; Dobbs, B.; Rout, J. E. *Nature* **1991**, *353*, 549.
(4) Heywood, B. R.; Mann, S. *J. Am. Chem. Soc.* **1992**, *114*, 4681.
(5) Qi, L.; Colfen, H.; Antonietti, M. *Angew. Chem., Intl. ed. Engl.* **2000**, *39*, 604.
(6) Morizot, A. P.; Neville, A. *Corrosion* **2000**, *56*, 638.
(7) Gabrielli, C.; Keddam, M.; Perrot, H.; Khalil, A.; Rosset, R.; Zindoune, M. *J. Appl. Electrochem.* **1996**, *26*, 1125.
(8) Pina, C. M.; Becker, U.; Risthaus, P.; Bosbach, D.; Putnis, A. *Nature* **1998**, *395*, 483.
(9) Therese, G. H. A.; Kamath, P. V. *Chem. Mater.* **2000**, *12*, 1195.
(10) Switzer, J. A. *Am. Ceram. Soc. Bull.* **1987**, *66*, 1521.
(11) Breyfogle, B. E.; Phillips, R. J.; Switzer, J. A. *Chem. Mater.* **1992**, *4*, 1356.
(12) Switzer, J. A.; Shane, M. J.; Phillips, R. J. *Science* **1990**, *247*, 444.
(13) Zhou, Y.; Phillips, R. J.; Switzer, J. A. *J. Am. Ceram. Soc.* **1995**, *78*, 981.
(14) Shirkhanzadeh, M. *J. Mater. Sci. Lett.* **1991**, *10*, 1415.
(15) Therese, G. H. A.; Kamath, P. V.; Subbanna, G. N. *J. Mater. Chem.* **1998**, *8*, 405.
(16) Xu, S.; Melendres, C. A.; Park, J. H.; Kamrath, M. A. *J. Electrochem. Soc.* **1999**, *146*, 3315.

10.1021/cm010098w CCC: $20.00 
Published on Web 09/18/2001

precipitate the inorganic material by direct oxidation of a soluble species in a low oxidation state to insoluble species in a higher oxidation state. Examples are the synthesis of $Tl_2O_3$ from $Tl^+$ solutions,[17] $MnO_2$ from $Mn^{2+}$ solutions,[18] and $PbO_2$ from $Pb^{2+}$ solutions.[19] The potentials used in such syntheses are usually too small to split water, and therefore, no acid is generated. When acidic protons are generated at the anode under high potential conditions, it is normally difficult to precipitate an inorganic material. We have exploited the instability of chelated $Ba^{2+}$ under acidic conditions to release free $Ba^{2+}$ cations in a bath of $SO_4^{2-}$ ions. As both the reactant species, $Ba^{2+}$ and $SO_4^{2-}$, do not undergo any direct oxidation and $BaSO_4$ is acid insoluble, the deposition of $BaSO_4$ takes place at the anode by electrogeneration of acid. Here we report the electrodeposition of $BaSO_4$ on polycrystalline stainless steel (SS) 304 electrodes, including the effect of current density and deposition time on crystallite orientation and morphology. To our knowledge, the use of electrogeneration of acid for electrodeposition of an inorganic material is being reported for the first time, as is the electrochemical preparation of $BaSO_4$.

## Experimental Section

All syntheses were carried out using a EG & G (PARC) Versastat Model IIA scanning potentiostat driven by Model 270 Electrochemistry Software. The $BaSO_4$ coatings were electrodeposited galvanostatically (current density, 10 mA/cm$^2$ or 40 mA/cm$^2$; time, 0.25−2 h) on stainless steel SS 304 flag electrodes (surface area, 4.5 cm$^2$) used as anodes in an undivided cell using a cylindrical Pt mesh electrode (surface area, 28 cm$^2$) as counter. A saturated calomel electrode was used as a reference electrode to measure the cell potential. The electrolyte used is a stabilized $BaSO_4$ bath, prepared by mixing equimolar (0.025 M) solutions of AnalaR grade (S. D. Fine Chemicals) $Ba(NO_3)_2$, disodium salt of EDTA, and $Na_2SO_4$ in a volume ratio of 1:20:1 in that order (final concentration $1.14 \times 10^{-3}$ M in $BaSO_4$) at pH 8 and allowed to stand in air for periods up to 3 h. No chemical precipitation was observed. Chemical precipitation was seen only on prolonged standing (12−18 h). These chemical (electroless) precipitations[20] yielded control samples of $BaSO_4$. All solutions were prepared using ion-exchanged (Barnstead Easypure) water with a specific resistance of 18.3 MΩ cm. After 0.25−2 h of deposition, during which aggressive oxygen evolution could be visibly observed at the working electrode, uniform white deposits could be seen on the anode. Due to dissolution of the stainless steel electrode simultaneously with $BaSO_4$ deposition, the weight of the $BaSO_4$ coating could not be monitored. Since the product of the electrodeposition does not ensue from an electrochemical reaction, Faradaic efficiencies are ill-defined and do not warrant measurement. Prior to deposition, the electrodes were cleaned in detergent and electrochemically as described elsewhere.[21] All coatings were characterized by powder X-ray diffractometry (XRD) by directly mounting the electrode on a Siemens D5005 diffractometer operated in reflection geometry. Data were collected with Cu Kα radiation using a continuous scan rate of 1° per minute ($2\theta$) or less and were then rebinned into $2\theta$ steps of either 0.02° or 0.05°, the former when the scattering was relatively strong. Three coatings were prepared under each experimental condition to verify the reproducibility of their structure. Scanning electron micrographs were recorded on a JEOL JSM 5600 LV directly from the coating on the substrate by mounting small pieces of the electrode on conducting carbon tape and sputter coating gold to improve conductivity.

## Results and Discussion

The solubility product of $BaSO_4$ is very small ($1.08 \times 10^{-10}$). Consequently, $Ba^{2+}$ and $SO_4^{2-}$ ions cannot be stabilized in a bath in the absence of a complexing agent. The disodium salt of EDTA ($H_2Y^{2-}$) was chosen for this purpose. As $H_2Y^{2-}$ does not contain any tetrahedral anion moiety and effectively functions as a dicarboxylate anion, it is not expected to have any structure- or growth-directing influence on $BaSO_4$ crystallites. Uchida et al.[22] have studied the effect of EDTA on the morphology of $BaSO_4$ crystallites obtained by the hydrothermal treatment of a Ba(EDTA) solution. They report changes in the crystallite morphology with Ba:EDTA ratio, suggesting that EDTA acts by the control of supersaturation of $Ba^{2+}$ ions rather than by bonding to specific crystal faces of $BaSO_4$. Therefore, we have maintained a constant Ba:EDTA ratio in all our syntheses in order to separate the effect of EDTA from that of electrochemistry.

Although EDTA and $Ba^{2+}$ form a 1:1 complex according to the equation

$$Ba^{2+} + H_2Y^{2-} \rightleftharpoons [Ba(H_2Y)]$$

a 20-fold excess of $H_2Y^{2-}$ was required to stabilize a $BaSO_4$ bath of 0.001 M concentration at pH 8 in an unbuffered solution. This complex dissociates at pH below 8. The acidification of the bath with a view to release $Ba^{2+}$ ions by dissociating the complex to achieve controlled growth of $BaSO_4$ crystallites was done for the first time using electrochemistry. The reaction carried out was the electrolysis of water leading to an oxygen evolution reaction (OER) according to the equation

$$2H_2O \rightarrow O_2 + 4H^+ + 4e^-$$

The measured cell potential (4.0−4.2 V) indicates OER to be the dominant reaction at the anode. Oxygen evolution causes a steep decline in the pH of the bath close to the anode, a phenomenon that we would like to refer to as electrogeneration of acid. This lowering of the pH causes dissociation of the complex and deposition of $BaSO_4$ on the anode.

The powder XRD pattern of a control sample of electroless $BaSO_4$ collected on an SS flag is shown in Figure 1. The profile could be fit by the Rietveld method as implemented in the XND Rietveld code (version 1.20)[23] using the published *Pnma* structure of $BaSO_4$.[24] Because the data are limited in signal and $2\theta$ range, only the profile and lattice parameters, the scale factor,

(17) Phillips, R. J.; Golden, T. D.; Shumsky, M. G.; Bohannan, E. W.; Switzer, J. A. *Chem. Mater.* **1997**, *9*, 1670.
(18) Preisler, E. *J. Appl. Electrochem.* **1989**, *19*, 559.
(19) Bullock, K. R. *J. Electroanal. Chem.* **1987**, *222*, 347.
(20) Kamath, P. V.; Subbanna, G. N. *J. Appl. Electrochem.* **1992**, *22*, 478.
(21) Corrigan, D. A.; Bendert, R. M. *J. Electrochem. Soc.* **1989**, *136*, 723.
(22) Uchida, M.; Sue, A.; Yoshioka, T., Okuwaki, A. *J. Mater. Sci. Lett.* **2000**, *19*, 1373.
(23) Bérar, J.-F., Program XND, ESRF, Grenoble, France. For more information see http://www.ccp14.ac.uk. Bérar, J.-F. *Proceedings of the IUCr Satellite Meeting on Powder Diffractometry*; Toulouse, France, July 1990; Bérar J,-F.; Garnier, P. II APD Conference, NIST (U.S.), Gaithersburg, Maryland, May 1992; Bérar J,-F.; Garnier, P. *NIST Special Publication* **1992**, *846*, 212.
(24) Hill, R. J. *Can. Mineral.* **1977**, *15*, 522; Inorganic Crystal Structure Database Entry 200112.

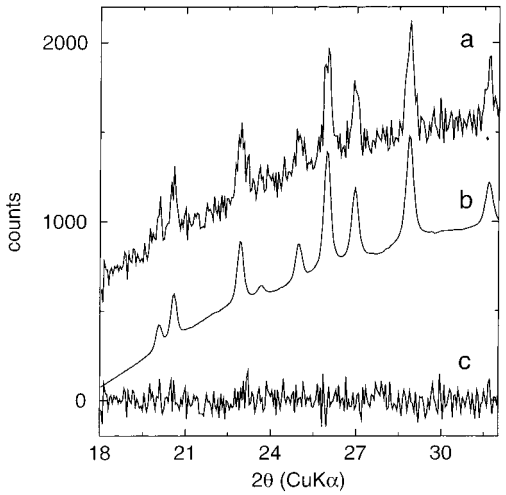


**Figure 1.** Observed (a), refined (b), and difference (c) powder XRD of the electroless $BaSO_4$ deposit.

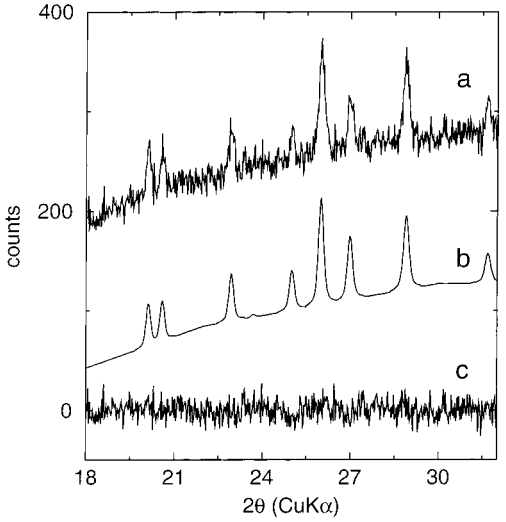


**Figure 2.** Observed (a), refined (b), and difference (c) powder XRD of the "slow" electrochemical deposit (10 mA/cm$^2$) of $BaSO_4$.

and positional parameters of the heavy atoms Ba and S were freed in the refinement. The sloping background in this and other XRD patterns arises because of the SS substrate. The background could be accounted for in the Rietveld fits using points selected on the background away from Bragg peaks that were then linear-interpolated to generate the entire background. The resultant fit, displayed in Figure 1 is quite satisfactory, considering the poor signal-to-noise ratio arising from the small sample quantity.

When the SS flag is an anode and the circuit is closed, the rapid formation of a white deposit is observed on the flag. Using galvanostatic conditions of 10 mA/cm$^2$ referred to hereafter as "slow" deposition, for a time of 1 h, we obtain the coating whose XRD pattern is displayed in Figure 2. A refinement of the diffraction profile using conditions similar to those used for the control sample reveals the coating to be $BaSO_4$.

Using a current of 40 mA/cm$^2$ (deposition time 1 h) yielded the coating whose XRD pattern is displayed in Figure 3. Using the same refinement strategy as in the previous cases resulted in a difference profile in which intensities due to (200), (210), and (211) reflections

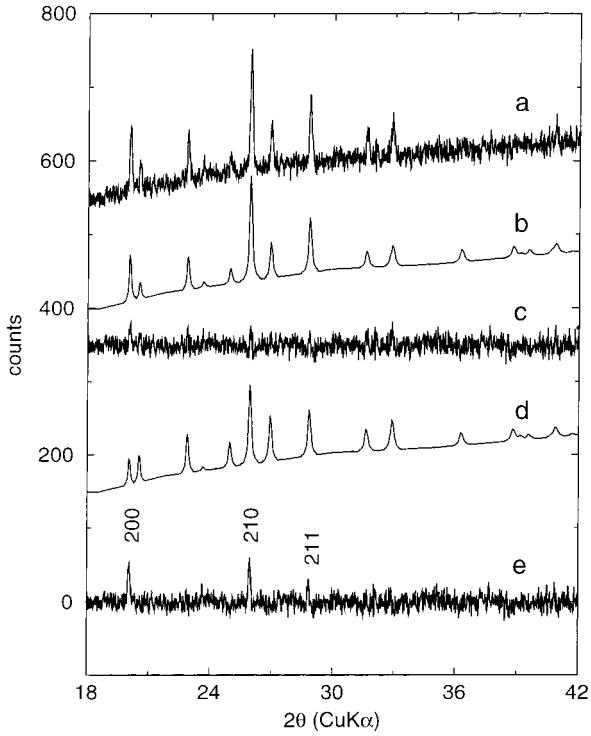


**Figure 3.** XRD profiles from the $BaSO_4$ deposit obtained using a current density of 40 mA/cm$^2$ and 1 h. (a) Observed, (b) refined with an *a* axis orientation, (c) resultant difference profile. Parts d and e represent the refinement and difference profile when orientation is not accounted for.

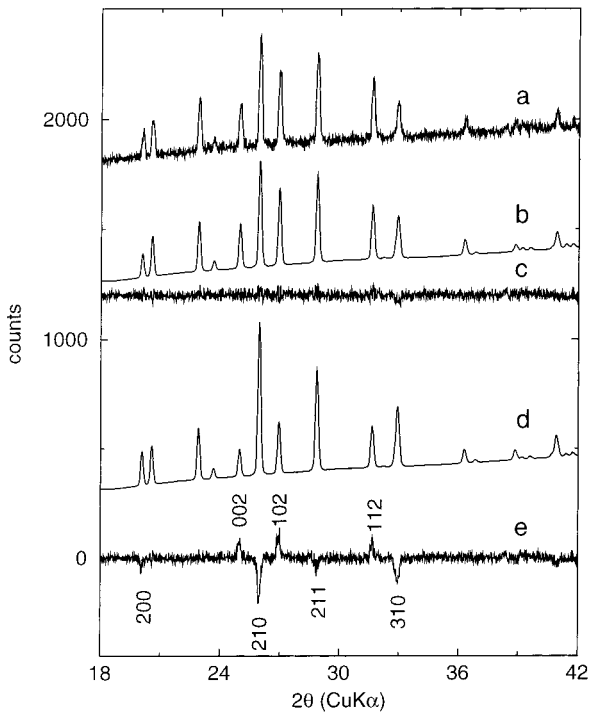


**Figure 4.** XRD profiles from the $BaSO_4$ deposit obtained using a current density of 40 mA/cm$^2$ and 2 h. (a) Observed, (b) refined with a *c* axis orientation, (c) resultant difference profile. Parts d and e represent the refinement and difference profile when orientation is not accounted for.

survived. This suggested a preferred orientation along the crystallographic *a* axis. Incorporating such a preferred orientation in the refinement yielded a satisfactory fit. To better quantify the preferred orientation, a

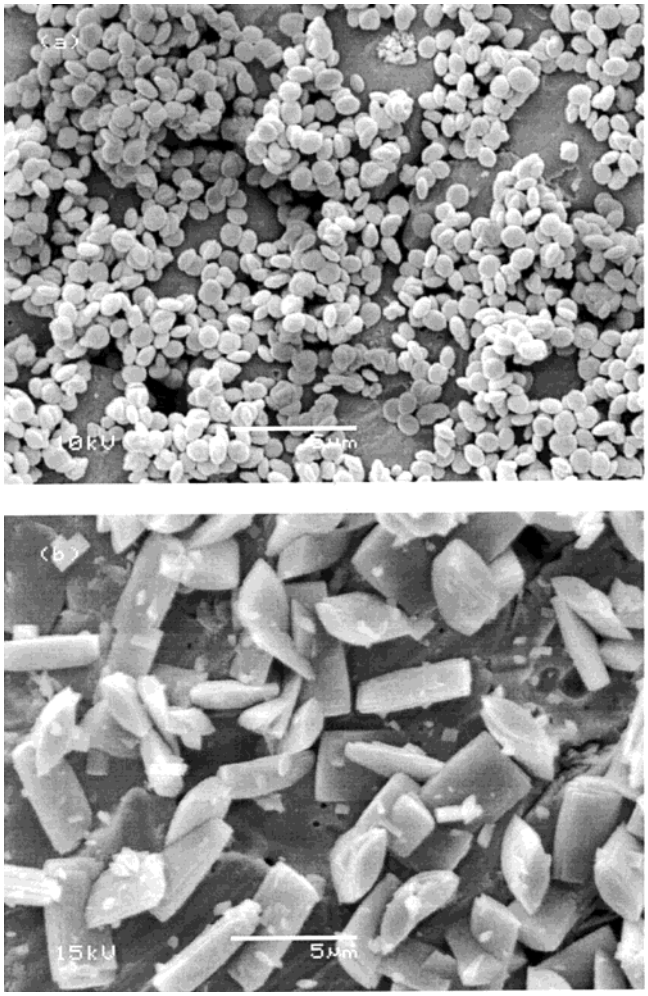


**Figure 5.** SEM images of (a) the electroless $BaSO_4$ precipitate and (b) the "slow" electrochemical deposit (10 mA/cm$^2$). The scale bars are 5 $\mu$m.

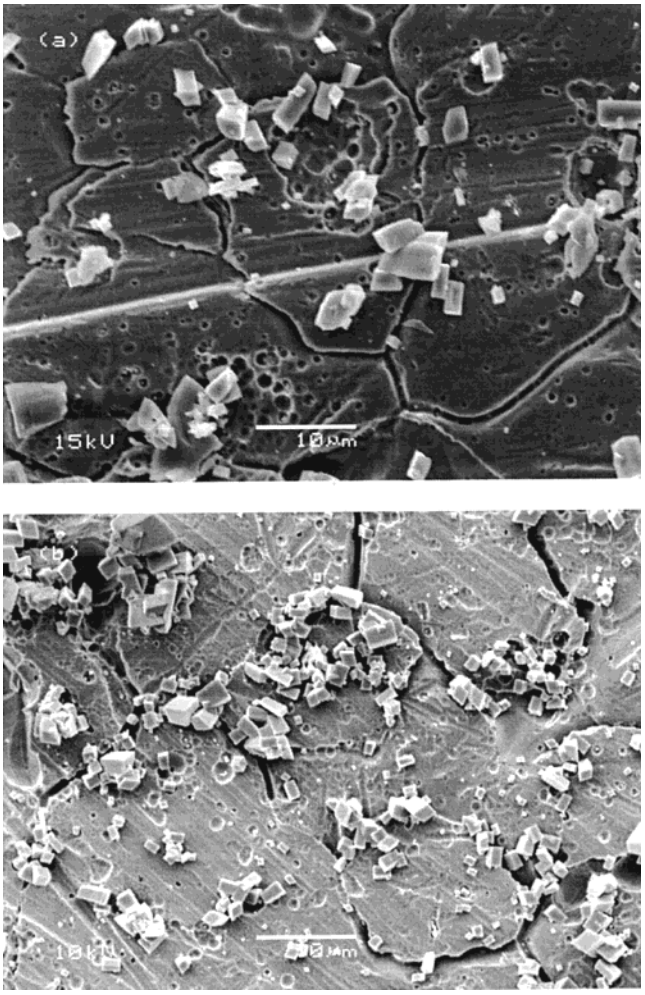


**Figure 6.** SEM images of $BaSO_4$ obtained at 40 mA/cm$^2$ for a deposition time of (a) 1 h and (b) 2 h. The scale bars are 10 $\mu$m.

further Rietveld refinement using the FULLPROF code[25] and the March preferred orientation function along the *a* axis was employed, wherein the refinable parameter varies from 1 (no orientation) to 0 (100% oriented). For this particular coating, this parameter refined to a value of 0.73.

At the same current density (40 mA/cm$^2$), a longer deposition time of 2 h yielded the coating whose XRD pattern is shown in Figure 4. The data in this case display better statistics. This enabled us to free all the positional parameters in the Rietveld refinement. Once again, a preferred orientation was suggested from certain systematics in the difference profile. This included an underestimation of the (002), (102), and (112) reflections and an overestimation of the (200), (210), (211), and (310) reflections, suggesting that the crystallites orient with their *c* axis perpendicular to the substrate. Incorporating a preferred orientation along the *c* axis in the refinement yielded a satisfactory fit. The FULLPROF refinement resulted in a value of 0.82 for the refinable parameter in the March function.

Typical scanning electron micrographs of the electrodeposited $BaSO_4$ coatings are compared with the control sample in Figures 5 and 6. The control experiment (electroless deposition) results in rounded crystallites ("peach"-like morphology in the terminology of ref 5), as shown in Figure 5a. This morphology is distinct from the orthorhombic crystallites that were obtained in a direct precipitation reaction by Antonietti and coworkers.[5] Under the "slow" electrochemical deposition conditions, the morphology is completely different, with the crystallites displaying significant facetting. The facetting is not uniform across the different crystallites, with rectangular, elliptical, and stepped faces being observed (see Figure 5b).

When the deposition is performed at 40 mA/cm$^2$, the crystallites do not grow uniformly on the surface (Figure 6), and large areas of the substrate are bare. This poor coverage can be attributed to the aggressive anodic dissolution of the substrate. The bare SS regions show pitting due to dissolution, and the $BaSO_4$ crystallites appear to grow along cracks on the substrate. While at low deposition times (1 h) the facetting is ill-defined (Figure 6a), the crystallites formed after 2 h are well-facetted orthorhombs.

Oriented growth of crystallites on a substrate can occur due to one or more of the following reasons: (i) Certain faces are intrinsically fast growing because they are less stable compared to others, and this might give rise to particles with a characteristic morphology and

(25) Rodríguez-Carvajal, J. Fullprof Rietveld Program, version 3.5, Laboratoire Leon Brillouin, Saclay, France. Also see the associated documentation.

therefore a propensity to orient with respect to the substrate. (ii) The substrate structure preferentially directs growth along a specific direction as in epitaxy. (iii) For reasons associated with the deposition technique.

We observe that neither the control electroless preparation nor the thin coating grown at 10 mA/cm$^2$ yield oriented $BaSO_4$ crystallites. This eliminates the first two factors as causes of oriented crystallization in the other coatings. There are many parameters that define the conditions of electrosynthesis: current density, pH of the bath, duration of deposition, and the nature of the electrode. Switzer and co-workers were able to switch the orientation of thin, electrodeposited $Cu_2O$ films on a SS substrate by varying the pH of the bath.[26] They have also reported enhanced orientation at higher current densities, consistent with our observations. In another study on $Tl_2O_3$ electrodeposition, they have reported enhanced orientation in thicker films.[17]

Although EDTA is not expected to affect the morphology of $BaSO_4$ crystallites, the control sample of electroless $BaSO_4$ comprises spheroids, which is a distinctly noncrystallographic morphology. This is in contrast to the tablet-like morphology expected of a direct precipitation reaction. We attribute this difference to the reduced kinetics of precipitation in the presence of EDTA. Enhancing the rate of crystallization by electrochemistry using progressively higher deposition currents leads to progressively well-facetted orthorhombs. These suggest that the observed morphological changes arise from the manner in which supersaturation is controlled, through control of pH, which in turn is influenced by the current density. Examples for morphological control through supersaturation are known, for example, from the geochemistry of magnesium-containing calcites.[27]

**Acknowledgment.** This reseach has been supported by the Department of Science and Technology, Goverment of India. We thank one of the reviewers for useful suggestions.

CM010098W

(26) Golden, T. D.; Shumsky, M. G.; Zhou, Y.; VanderWerf, R. A.; Van Leeuwen, R. A.; Switzer, J. A. *Chem. Mater.* **1996**, *8*, 2499.

(27) Devery, D. M., Ehlmann, A. J. *Am. Mineral.* **1981**, *66*, 592.